INTEGRATING LASER SCANNING WITH DISCRETE ELEMENT MODELING FOR IMPROVING SAFETY IN UNDERGROUND STONE MINES

JUAN J. MONSALVE
M.S. MINING ENGINEERING
MINING AND MINERALS ENGINEERING DEPARTMENT
VIRGINIA TECH

THE DEPART

CONTENT

1. INTRODUCTION

"The guidelines for pillar and roof span design are empirically based; their validity, therefore, is restricted to rock conditions, mining dimensions, and pillar stresses that are similar to those included in this study. These guidelines should be applicable to the majority of stone mines in the Eastern and Midwestern United States. If pillars need to be designed that are outside the validity of these design guidelines, the advice of rock engineering specialists should be sought." (NIOSH, 2011)

Partially benched pillar that failed along two angular discontinuities. Width-to-height ratio is 0.58 based on full benching height and average pillar stress is about 4 percent of the UCS.

Pillar that has an original width-to-height ratio of 1.7 failed by progressive spalling. Thin weak beds are thought to have contributed to the failure. The average pillar stress was about 11 percent of the UCS prior to failure.

(Esterhuizen, Dolinar, & Ellenberger, 2008)

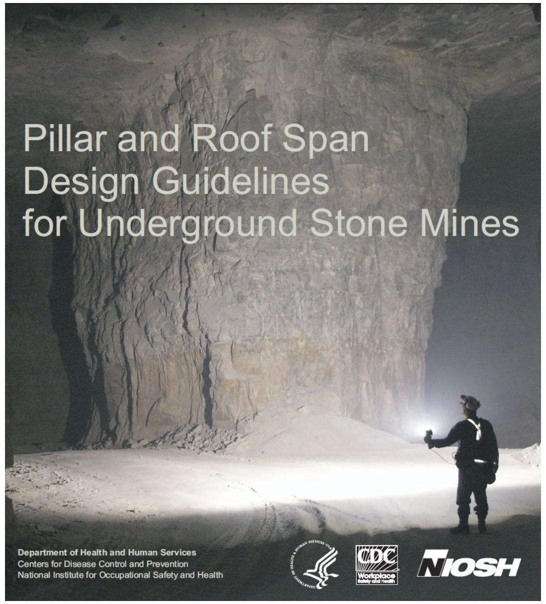

2. OBJECTIVE

To develop and implement a methodology that integrates laser scanning technology along with Discrete Element Modeling as tools for characterizing, preventing, and managing structurally controlled instability that may affect large-opening underground mines from a risk perspective.

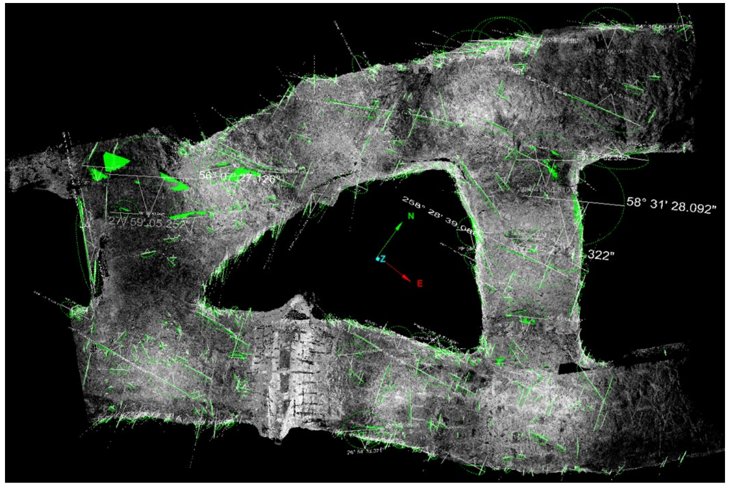

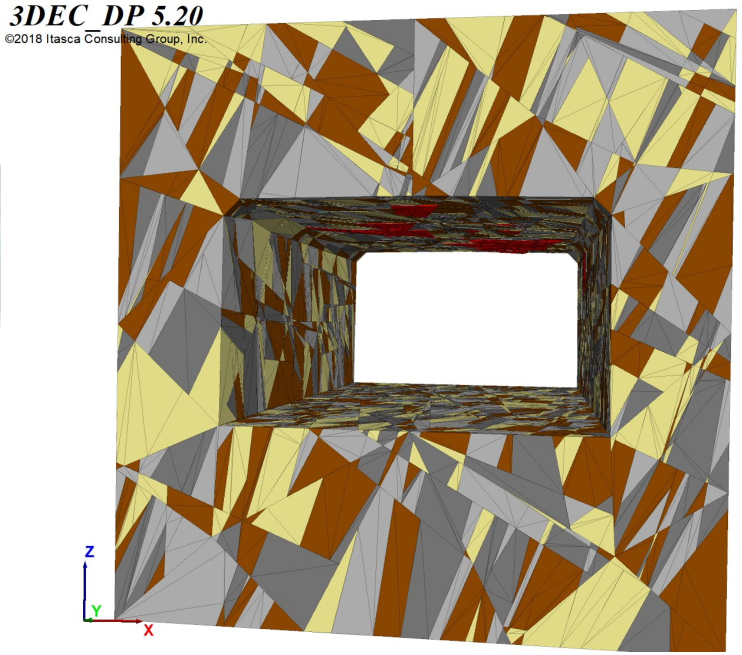

3. CASE STUDY MINE

3. CASE STUDY MINE

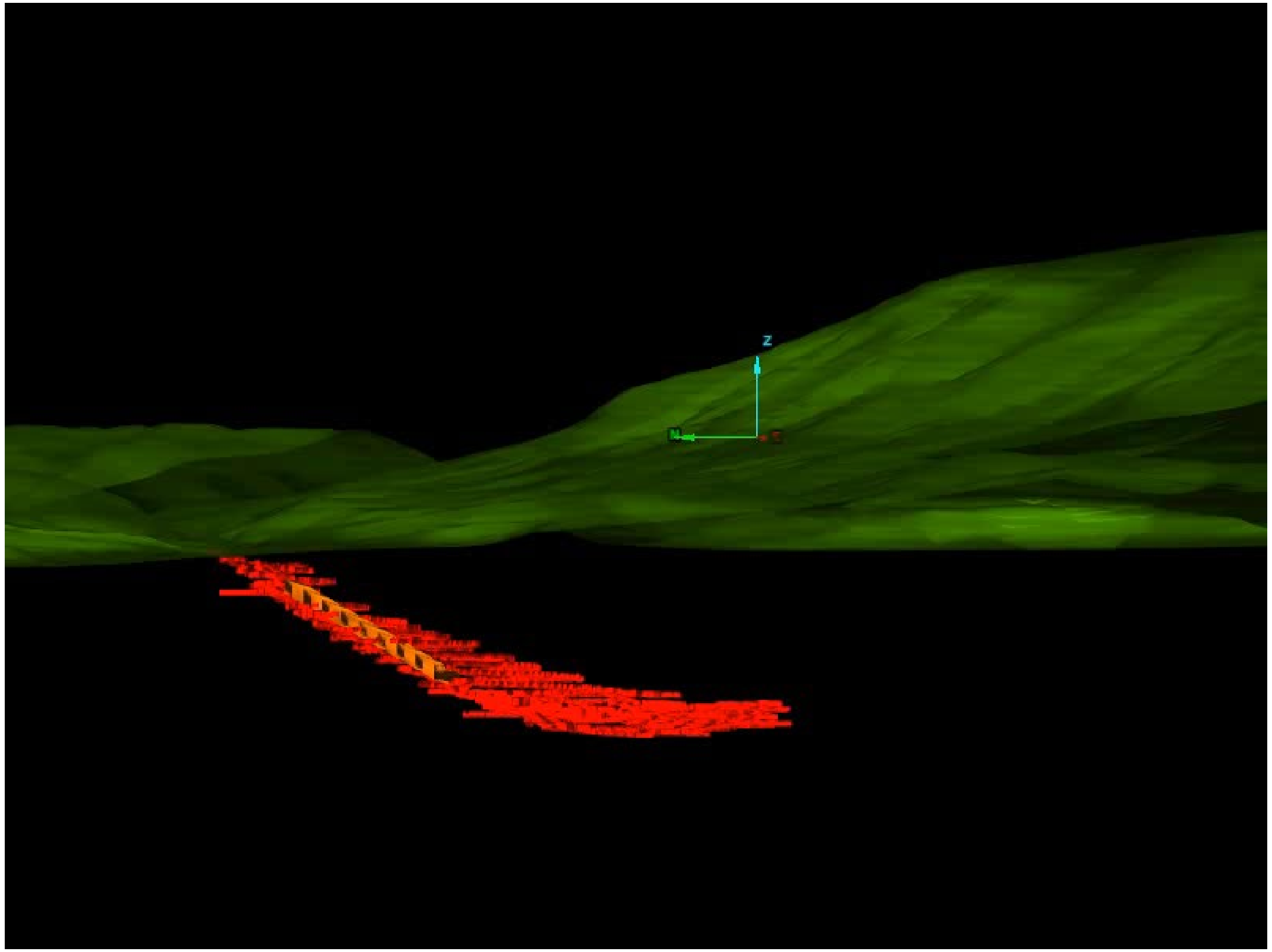

3. GEOTECHNICAL CONDITIONS

3. GEOTECHNICAL CONDITIONS

Description	jointing pattern where at least four joint sets were well defined
	observed wide-joint spacing, generally ranging from 0.6 m to 2 m,
	amount of fallen blocks observed on the floor with cubical and tabular shapes,
	joint surfaces defined as mostly closed, flat and smooth, with a JRC ranging from 2 to 4, completely dry and fresh,
	other geological structures, such as faults and contacts, that could generate a rock fall in the absence of the required support

Rock Mass Classification		
RMR	70 - 75	Good
Q	8 - 20	Fair
GSI	≈ 75	

3. GEOTECHNICAL CONDITIONS

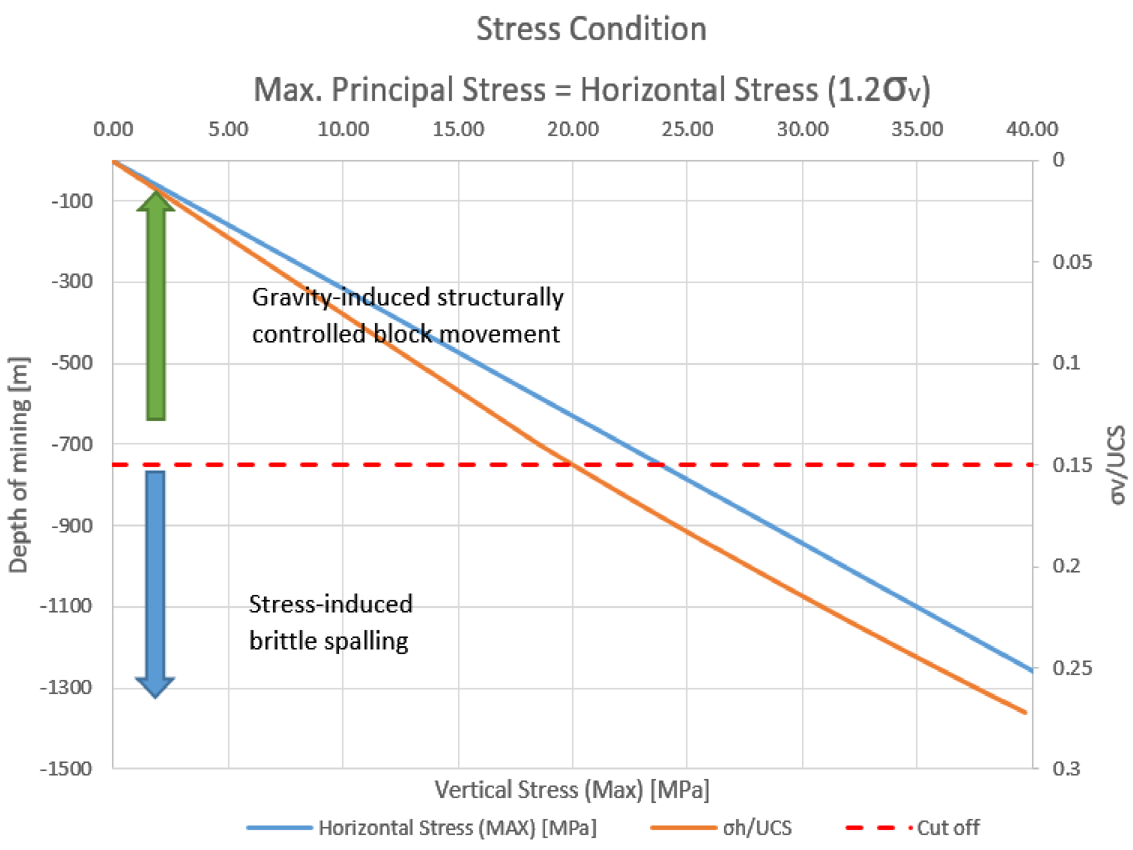

$$\sigma_v = \gamma h = 2.7\, {}^{ton}/_{m^3} * 9.81\, {}^{m}/_{s^2} * 700m \qquad \sigma_v = 18.5\ MPa$$

Lithology	Density (ton/m3)		UCS (MPa)		Brazilian Tensile Strength (MPa)		Young's Modulus (GPa)	
	Mean	SD	Mean	SD	Mean	SD	Mean	SD
Hanging Wall	2.69	0.01	163.74	37.84	11.96	3.14	61.02	6.79
Ore Body	2.69	0.01	159.20	21.25	6.30	1.99	64.11	2.37
Footwall	2.72	0.01	217.29	36.12	13.72	2.62	61.43	3.15

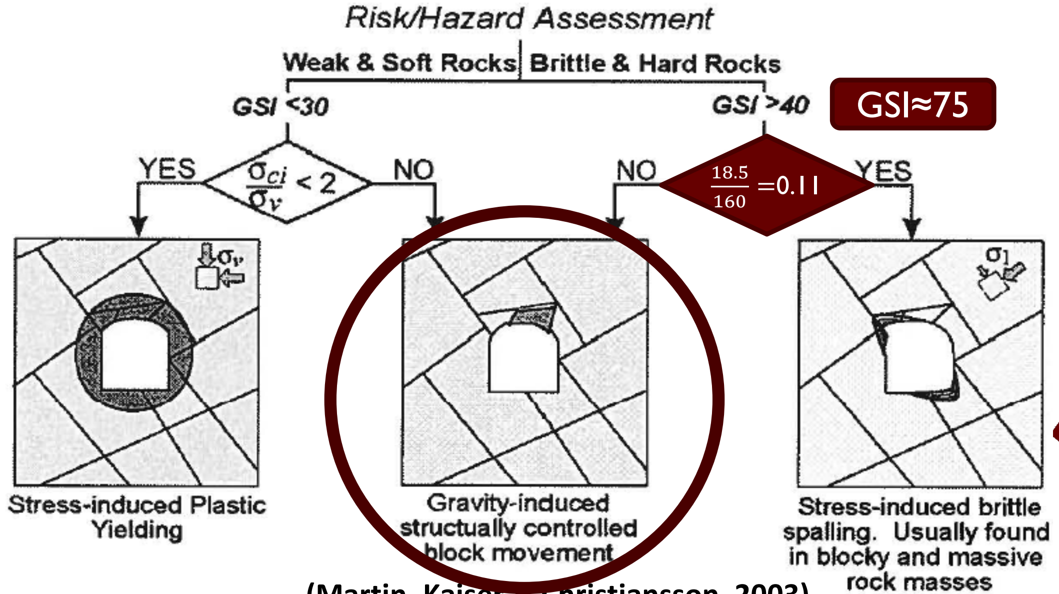

(Martin, Kaiser & Christiansson, 2003)

4. METHODOLOGY

1. Laser Scanning
2. Virtual Discontinuity Mapping
3. DFN Generation
4. Preliminary 3DEC Models
5. Stochastic 3DEC Modeling

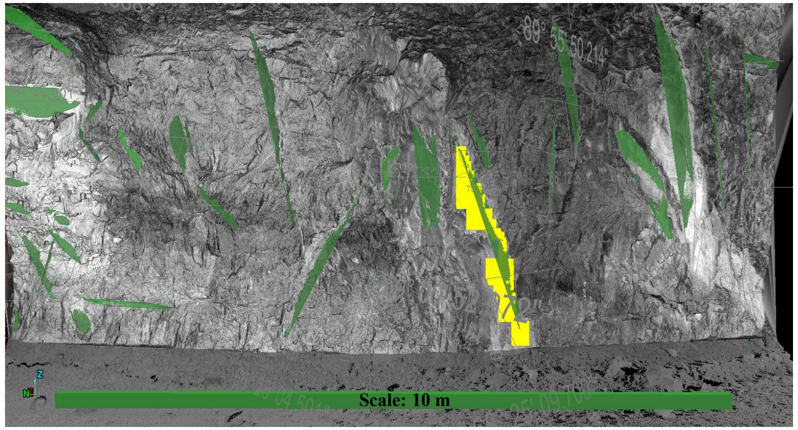

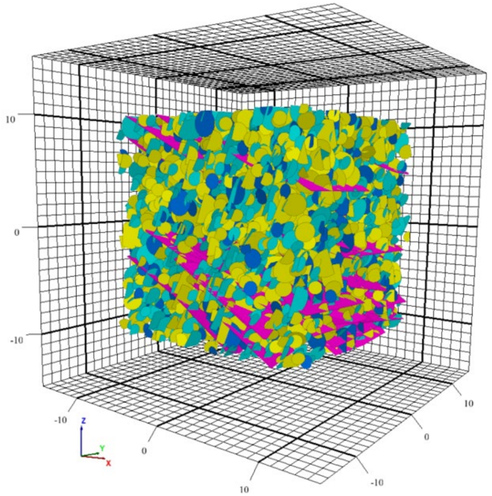

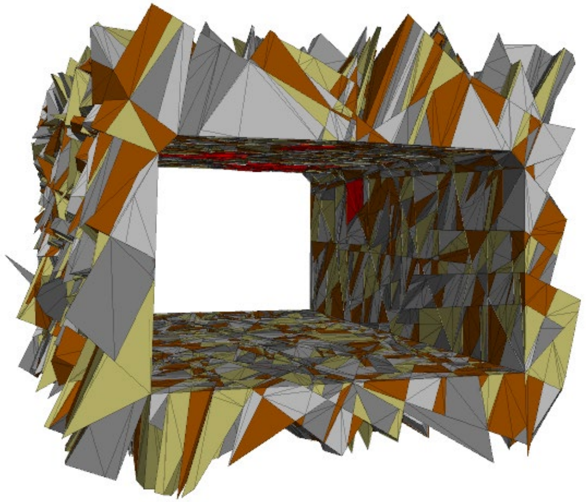

5. RESULTS

5.1. LASER SCANNING - EQUIPMENT

FARO Focus 3D
Maximum Resolution 710.7 Million of points / scan
Purchased in 2011
Maximum Measurement Speed 976,000 pts/s
Ranging error ± 2mm @ 10 m
Internal Compass
No integrated GPS

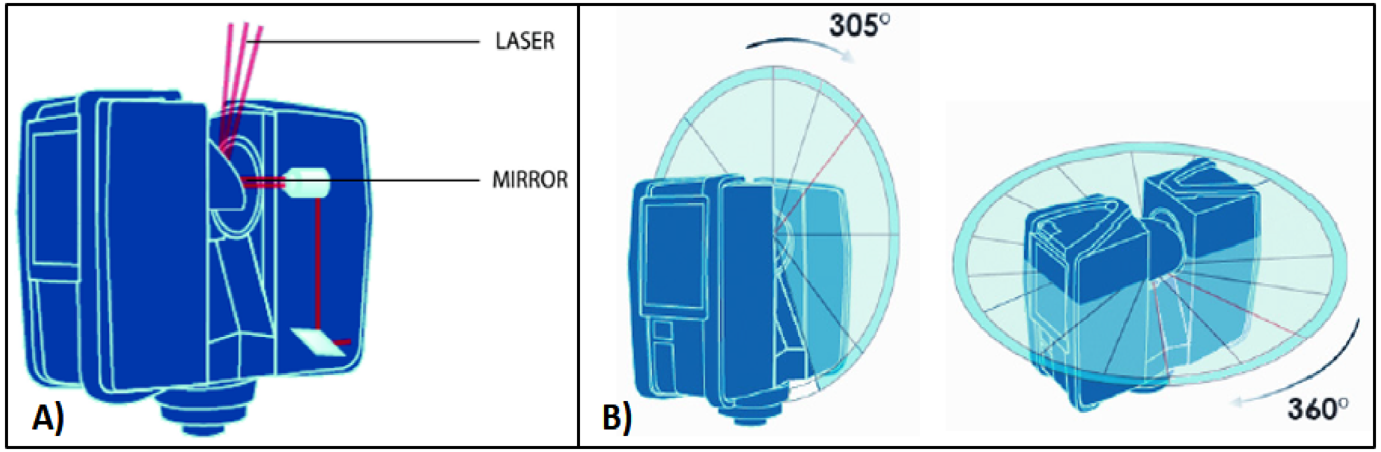

5.1. LASER SCANNING – STATIONS LOCATION

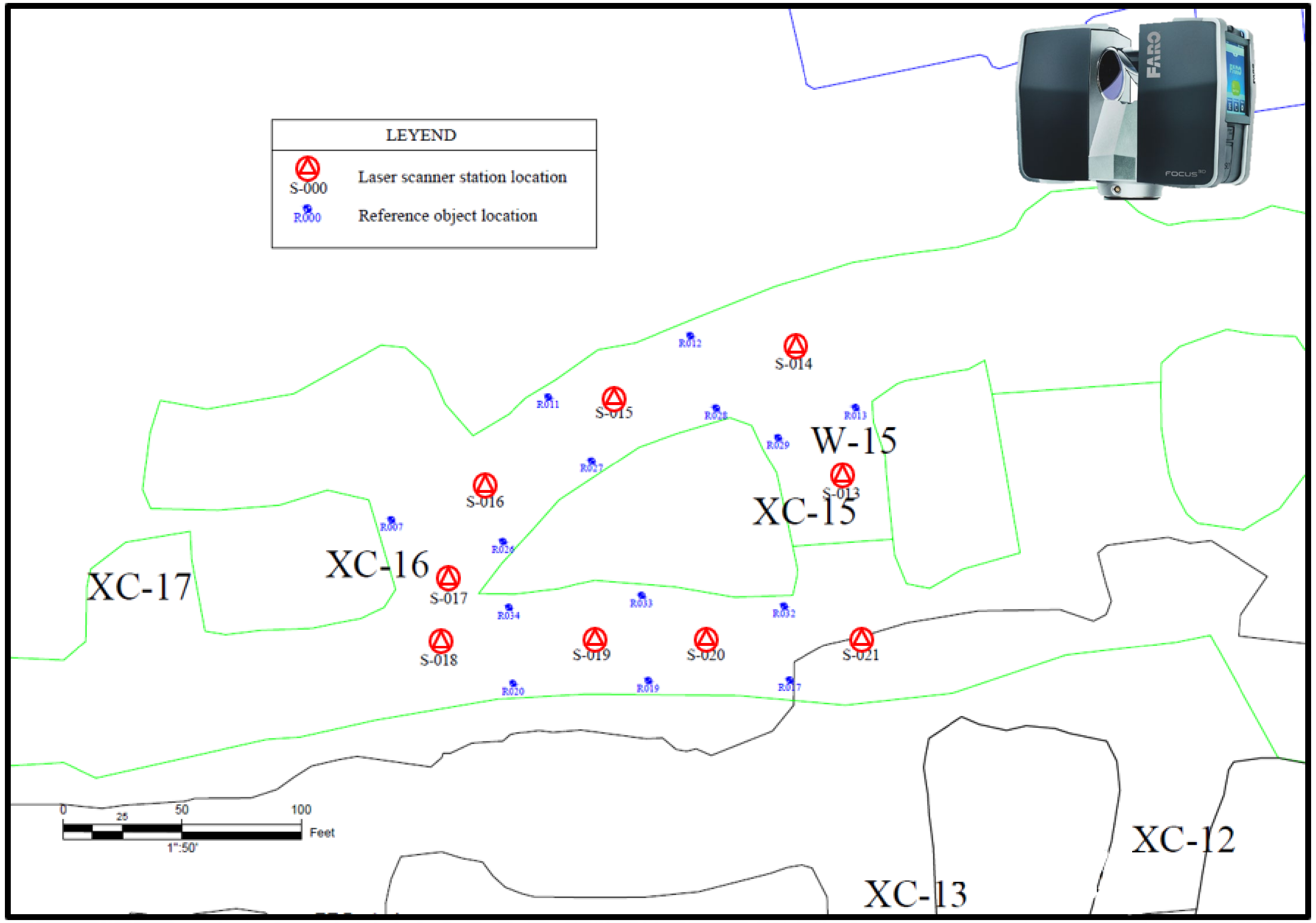

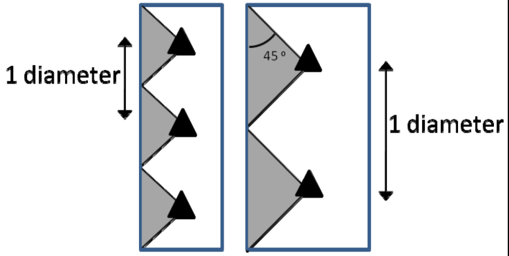

(Fekete, 2010)

13 m Between stations

6.5 m Between stations and reference objects


Z
E
N

5.2. VIRTUAL DISCONTINUITY MAPPING

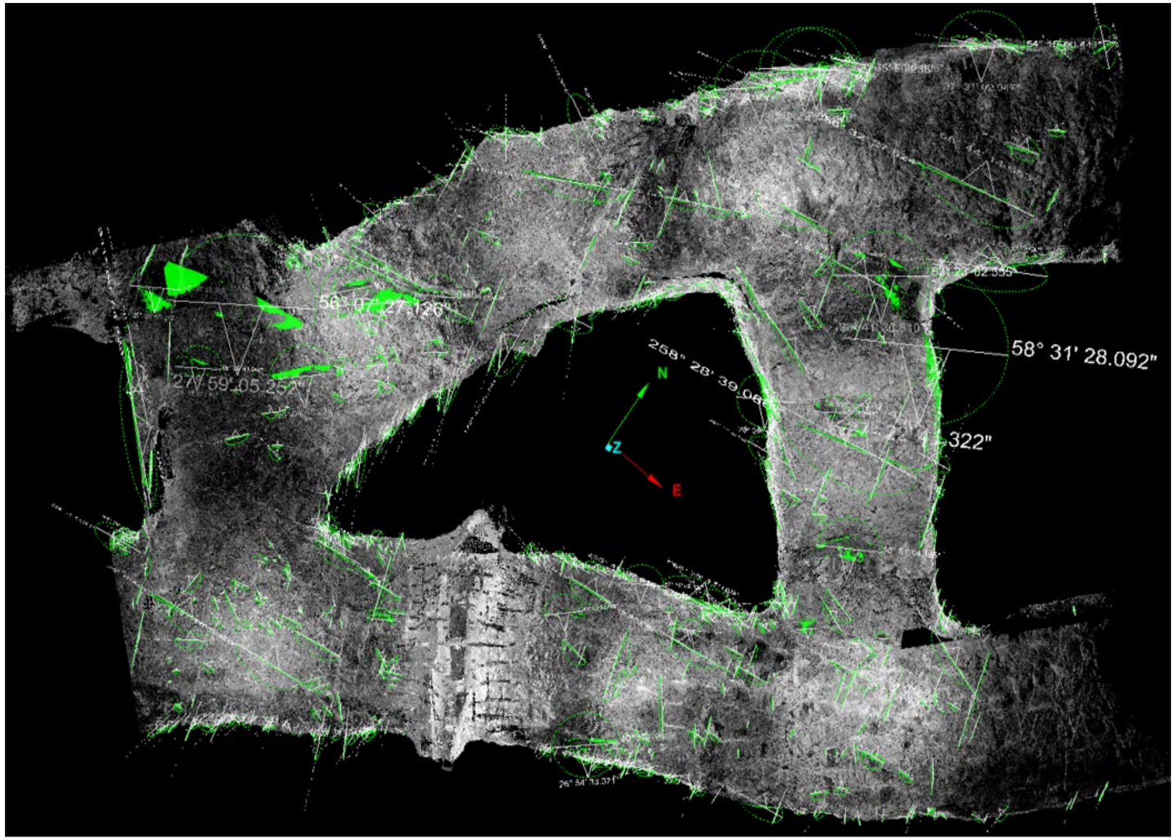

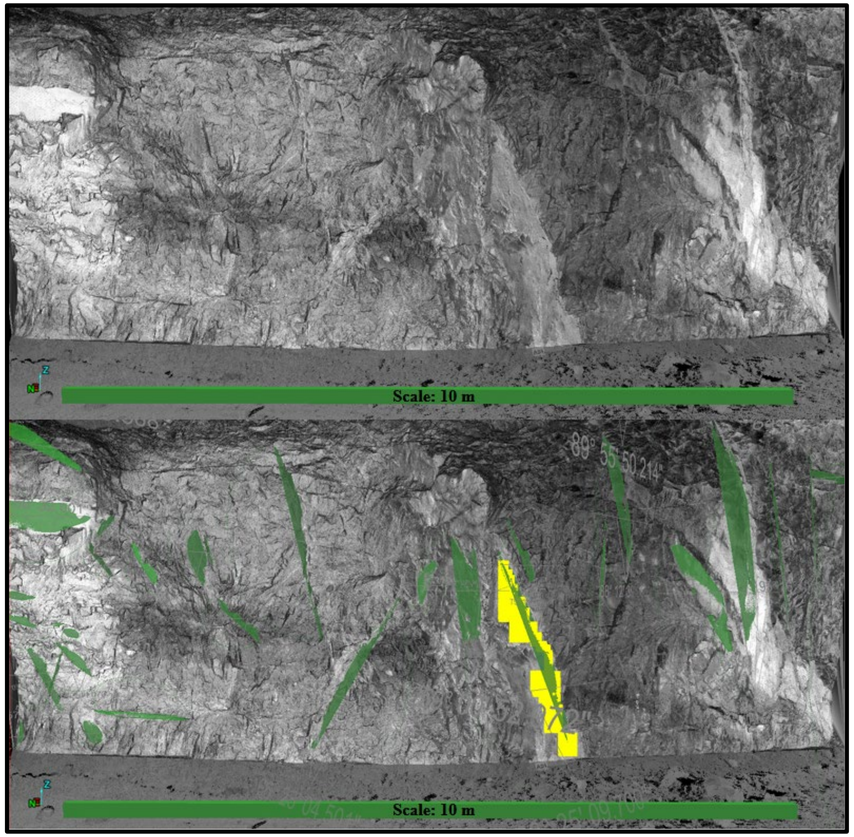

MAPTEK I-Site

5.2. VIRTUAL DISCONTINUITY MAPPING - RESULTS

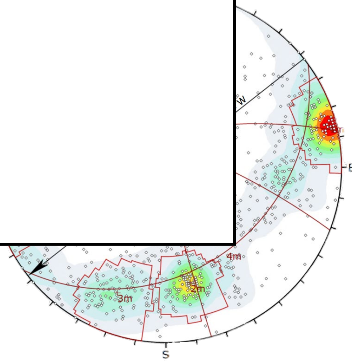

Trace Length

SET 1 SET 2 SET 3 SET 4

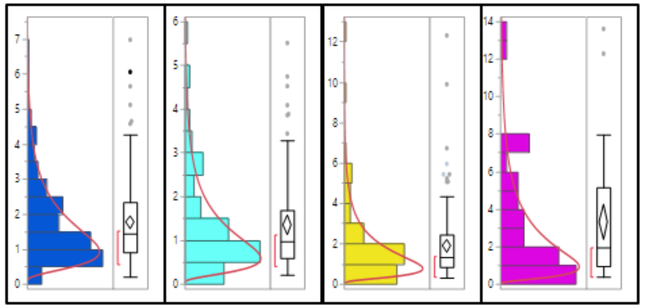

SET 1	SET 2	SET 3	SET 4
Log-normal	Log-normal	Log-normal	Log-normal
μ=0.35373	μ=0.31809	μ=0.019	μ=0.77886
σ= 0.65988	σ= 0.77215	σ= 0.74999	σ= 0.93466

Fracture Density P_{10}

SET 1 SET 2 SET 3 SET 4

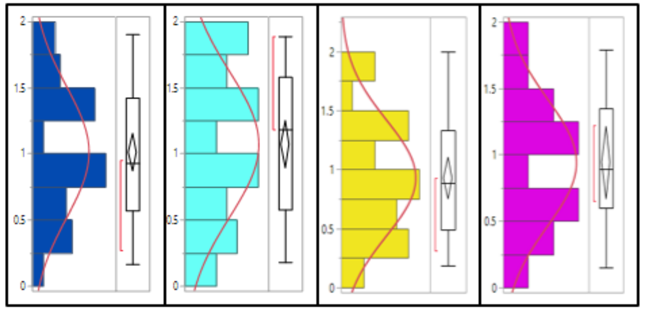

SET 1	SET 2	SET 3	SET 4
Normal μ=1.011 σ= 0.495	Min=0.18 Q2=0.576 Median=1.180 Q3=1.577 Max=1.883	Normal μ=0.928 σ= 0.492	Normal μ=0.941 σ= 0.477

5.3. DISCRETE FRACTURE NETWORK (DFN) GENERATION

A DFN is a three-dimensional geometric representation of a geological structure based on statistical information of its characteristics measured on the field (Pierce, 2017).

- Orientation
- Fracture Density
- Joint Size

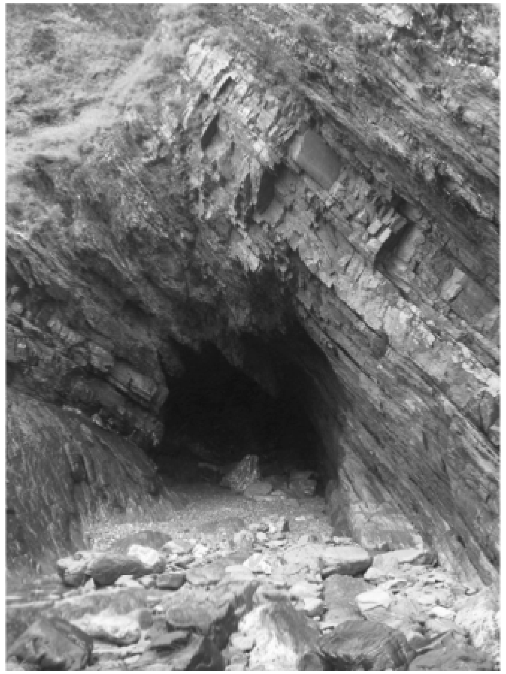

Exposure 4. Coastal cave in a layered rock mass, UK

(Hudson & Xia, 2015)

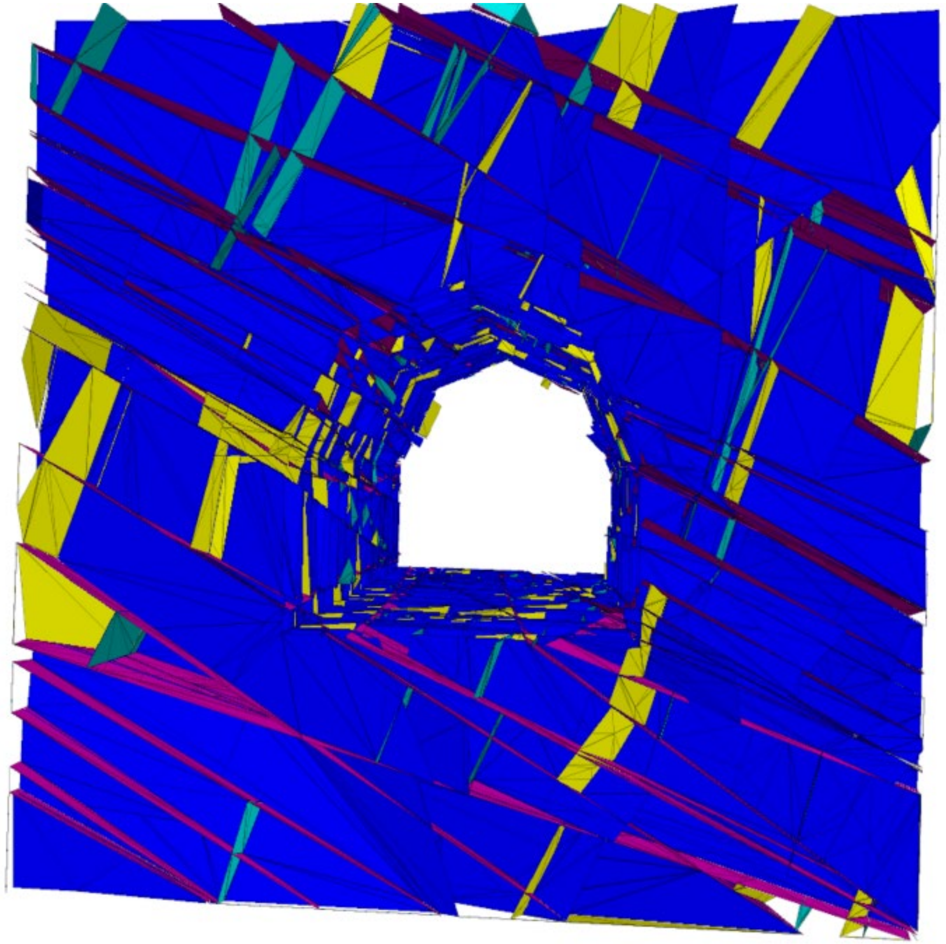

5.4. PRELIMINARY NUMERICAL MODEL (3DEC)

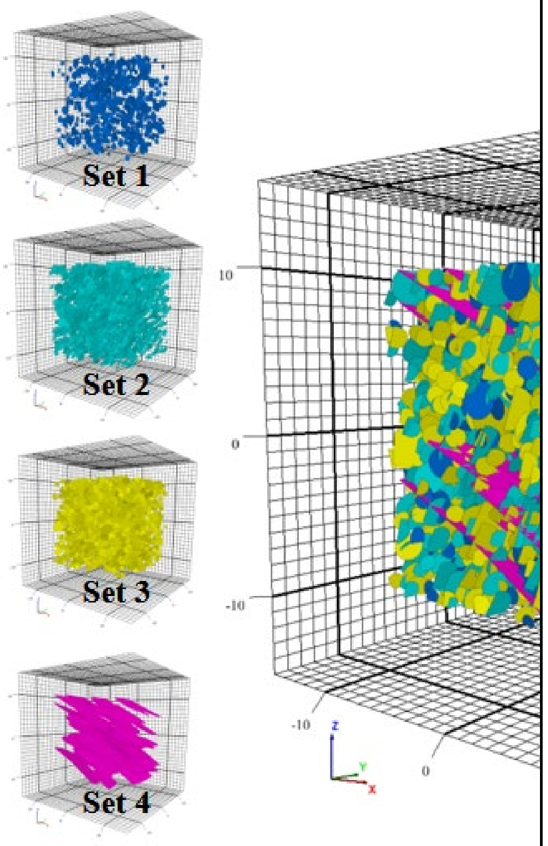

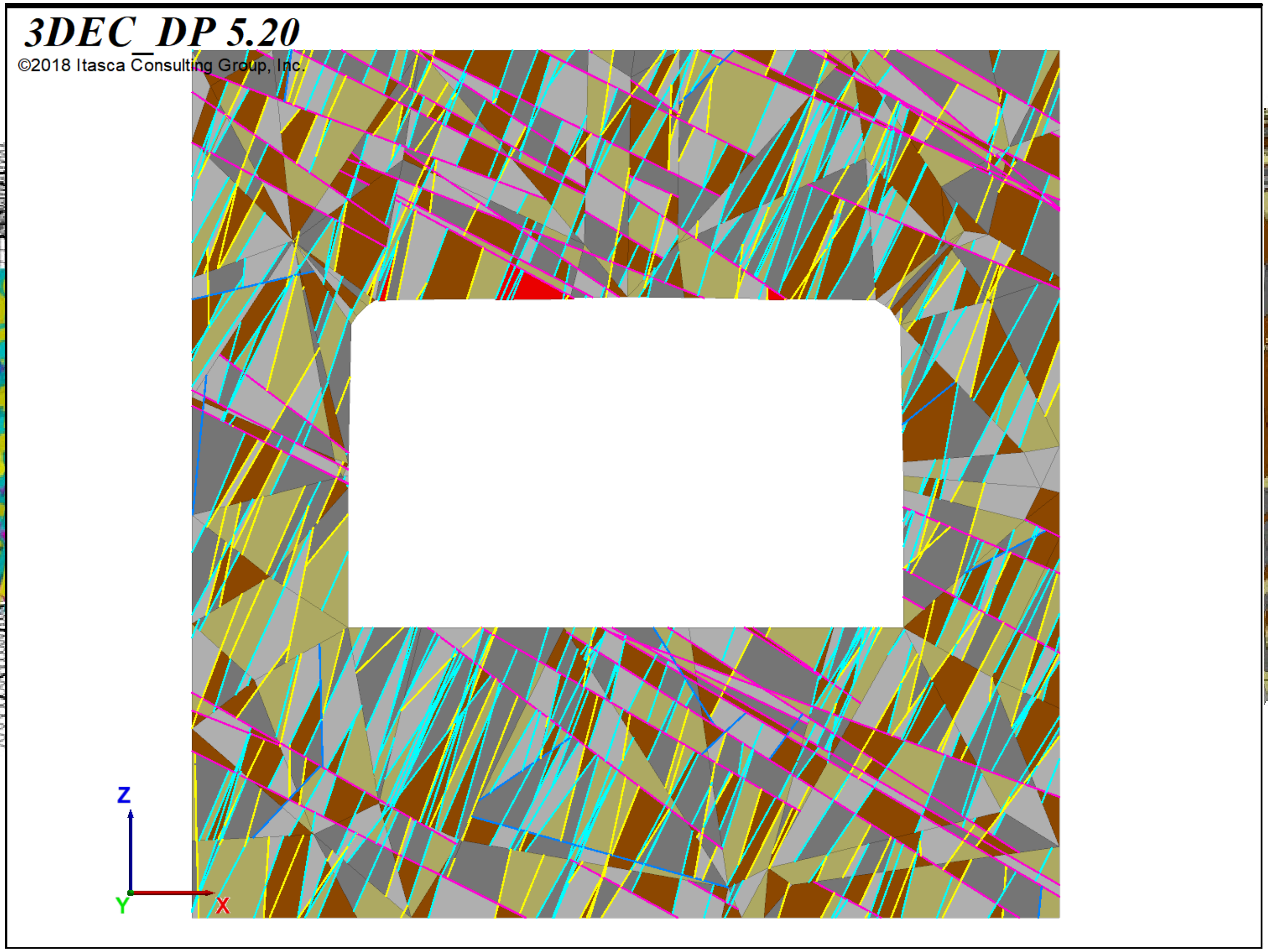

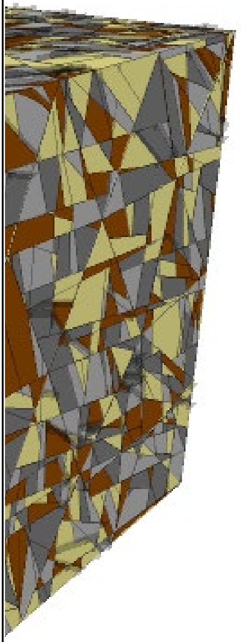

5.4. PRELIMINARY NUMERICAL MODEL (3DEC)

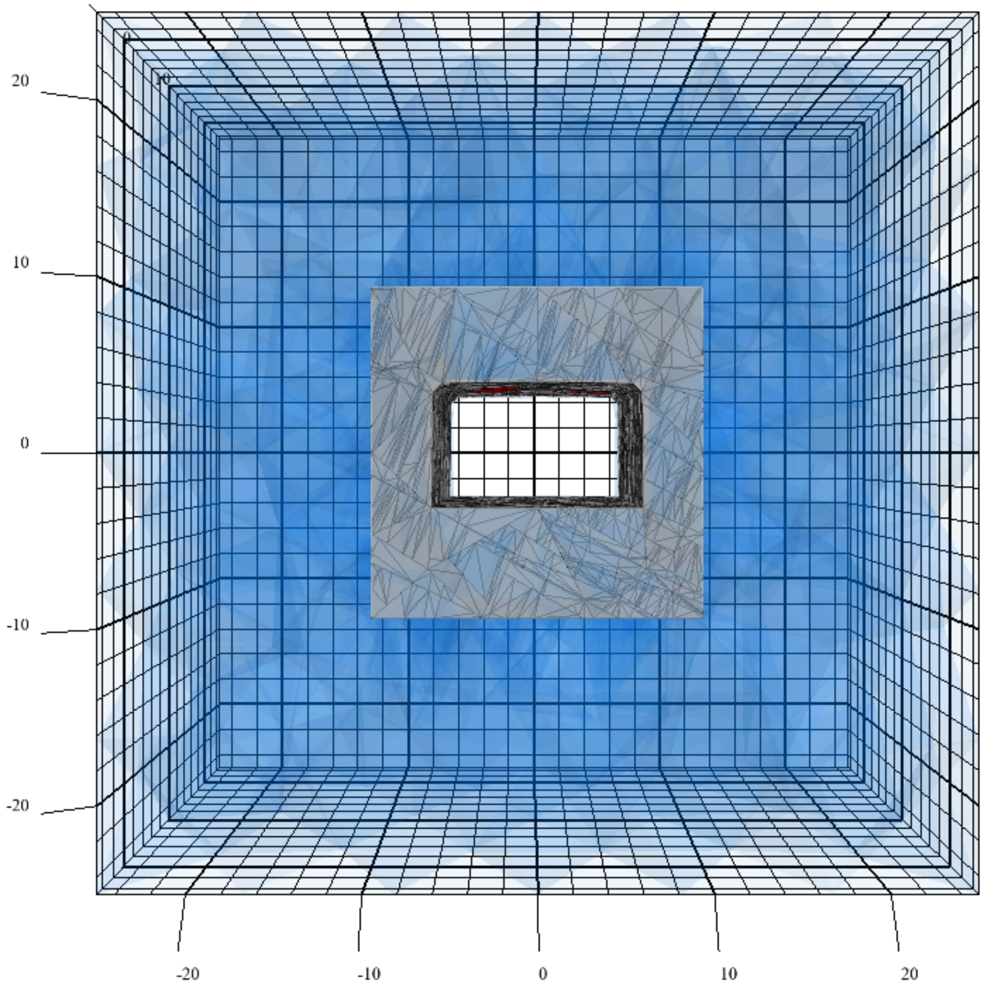

- Inner section: Fractured rock mass
  - Cut by 4 DFNs (20 m x 20 m x 20 m)
- External section: Massive rock mass – Fixed blocks
- Excavation Dimensions
  - 20 m length
  - 12.8 m width
  - 7.6 m height
- Stresses @ 700 m deep
  - $\sigma_v = 18.54\ MPa$
  - $\sigma_h = 20.39\ MPa$

5.4. PRELIMINARY NUMERICAL MODEL (3DEC)

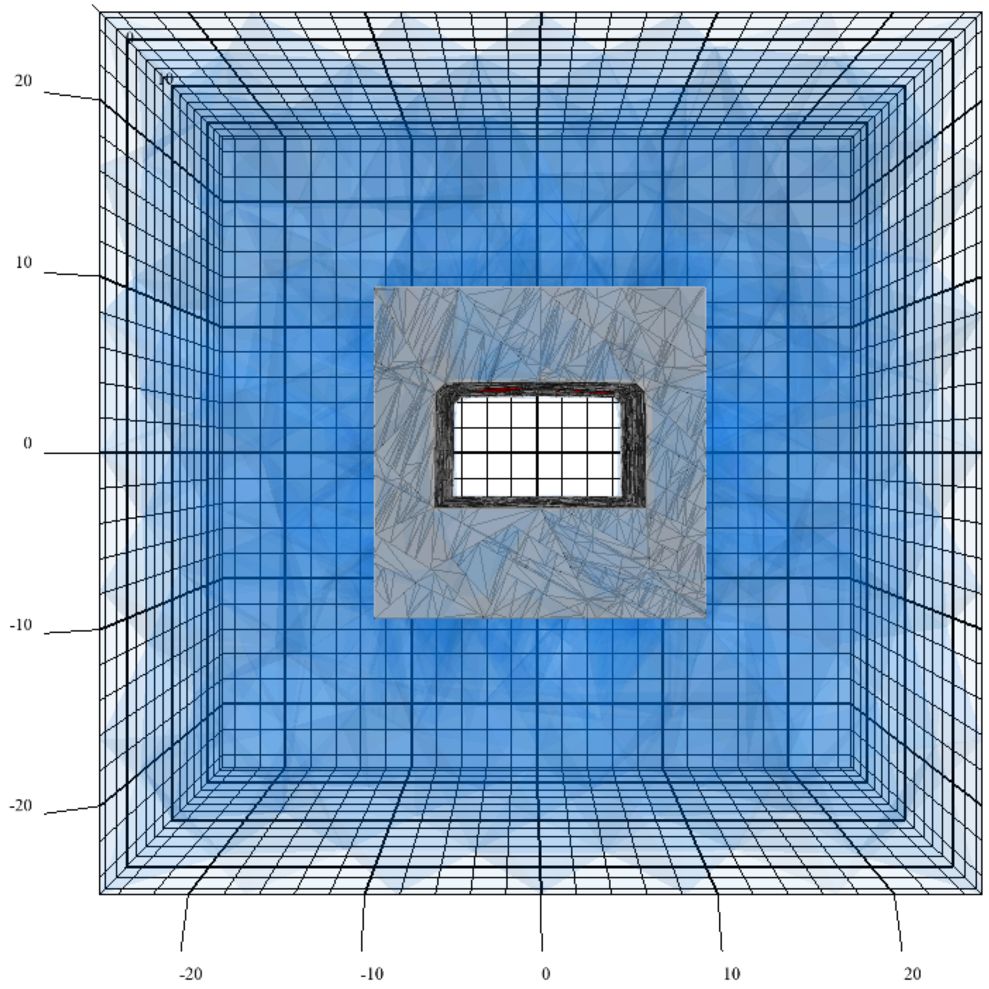

- Rigid block model (Blocks assumed infinitely stiff)
- Rock Density = 2.7 ton/m^3
- Mohr - Coulomb Constitutive Model for Fractures
  - $\varphi = 30^{\circ}$ & $cohesion = 0$
  - $J_{ks} = 30\ MPa/mm$
  - $J_{kn} = 300 MPa/mm$ (Bandis, Lumsden, & Barton, 1983)
- 1000 Initial cycles
- Progressive excavation (6 stages) – 5 m sections
  - 1000 cycles elastic – Damping
  - 1000 cycles plastic
  - time step of 3.81x10^{-6} s

5.4. PRELIMINARY NUMERICAL MODEL (3DEC)

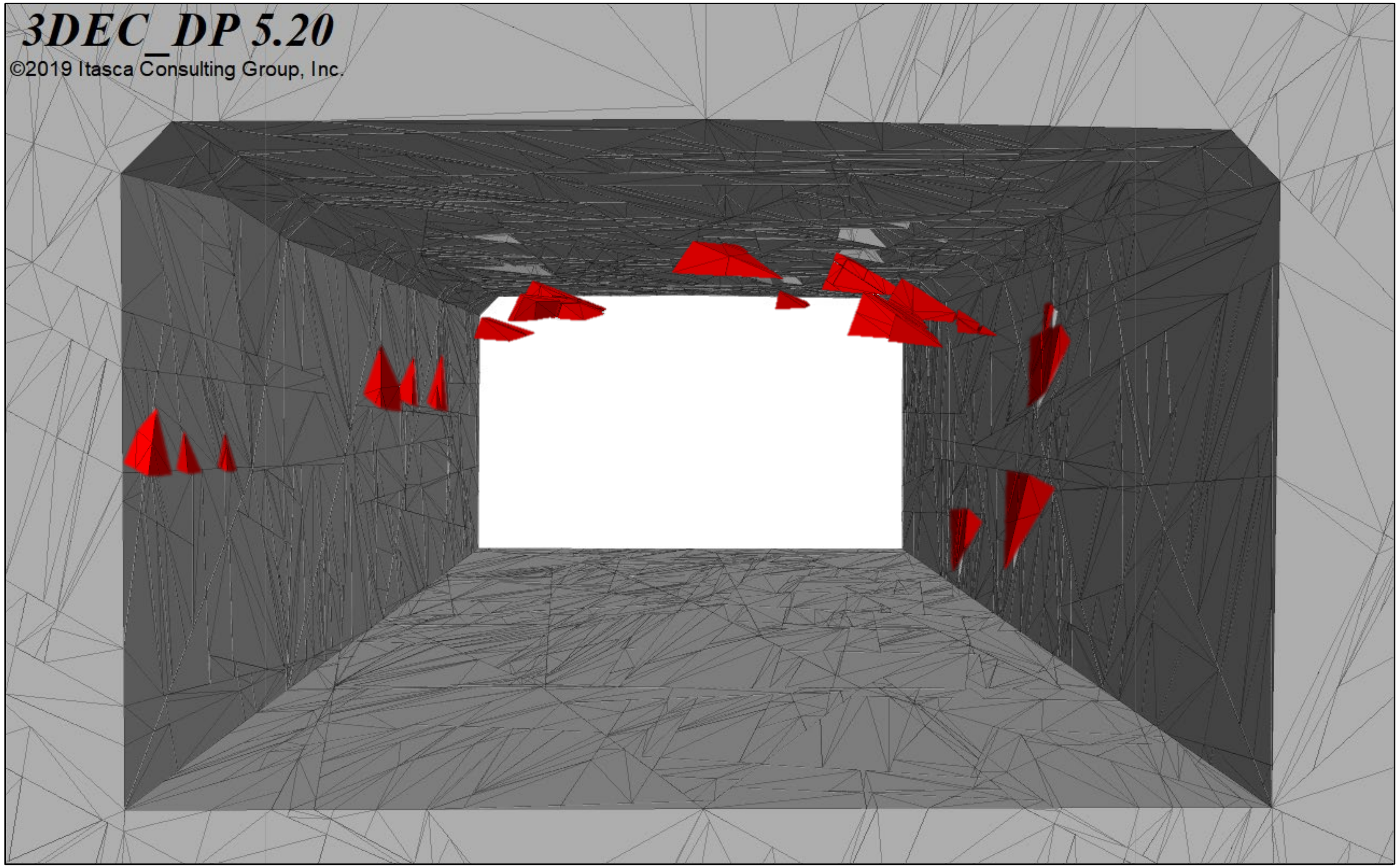

5.5. STOCHASTIC DISCRETE ELEMENT MODEL

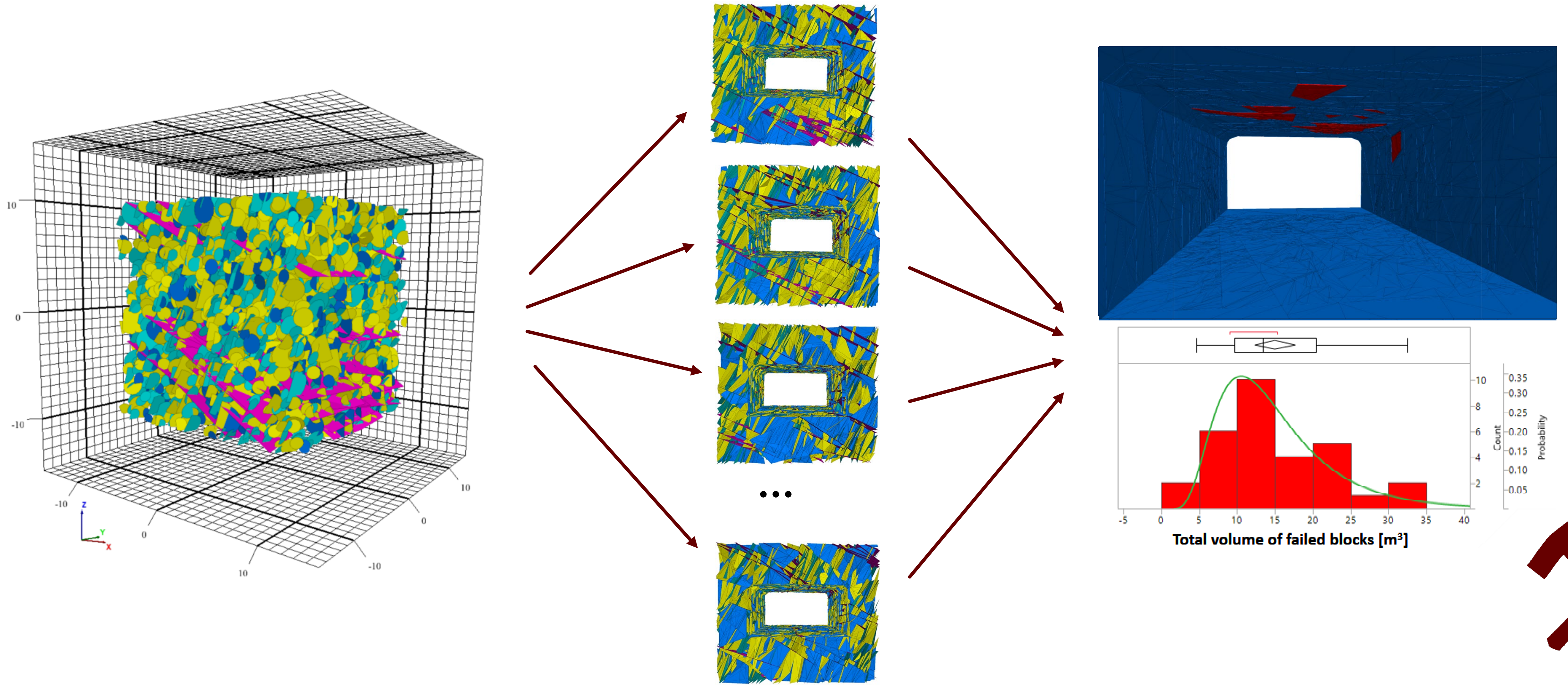

5.5. STOCHASTIC DISCRETE ELEMENT MODEL - RESULTS

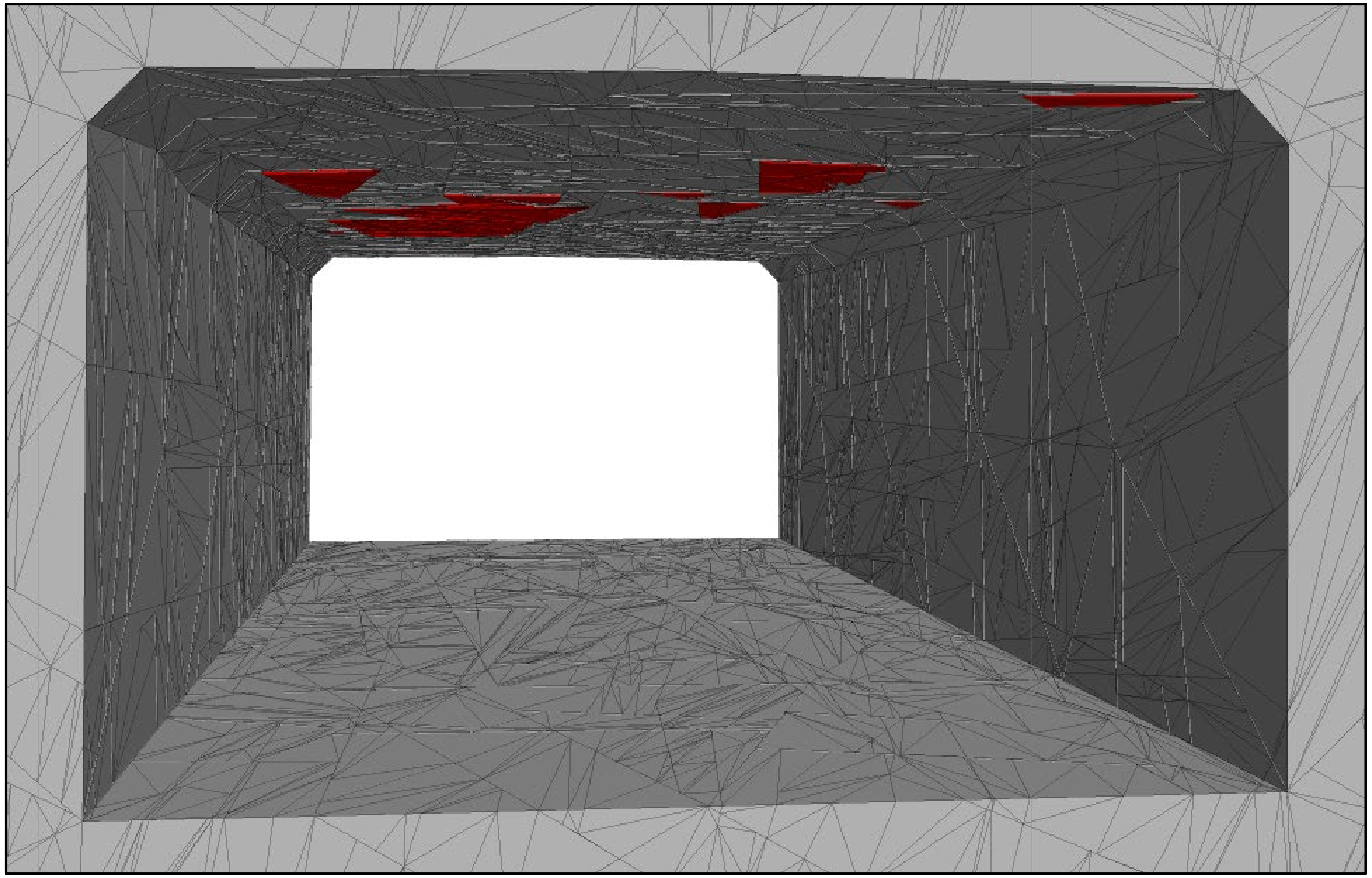

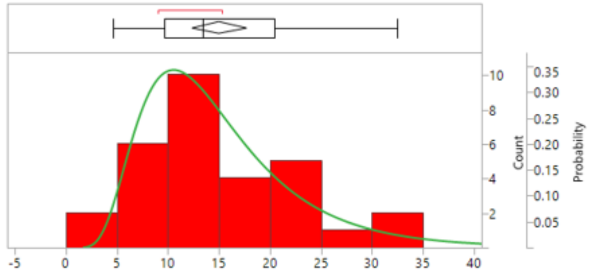

Total volume of failed blocks [m³]

Summary Statistics	
Distribution	Log-Normal
Mean	2.60
Standard Deviation	0.49

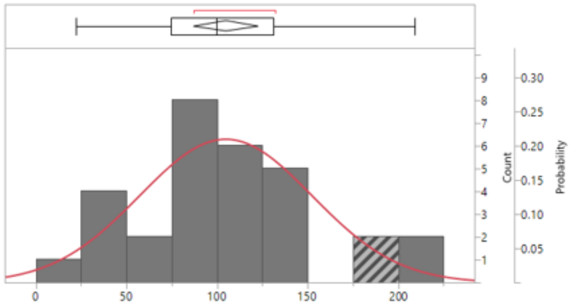

Number of failed blocks [m³]

Summary Statistics	
Distribution	Normal
Mean	104.87
Standard Deviation	47.58

5.6. MODEL VALIDATION

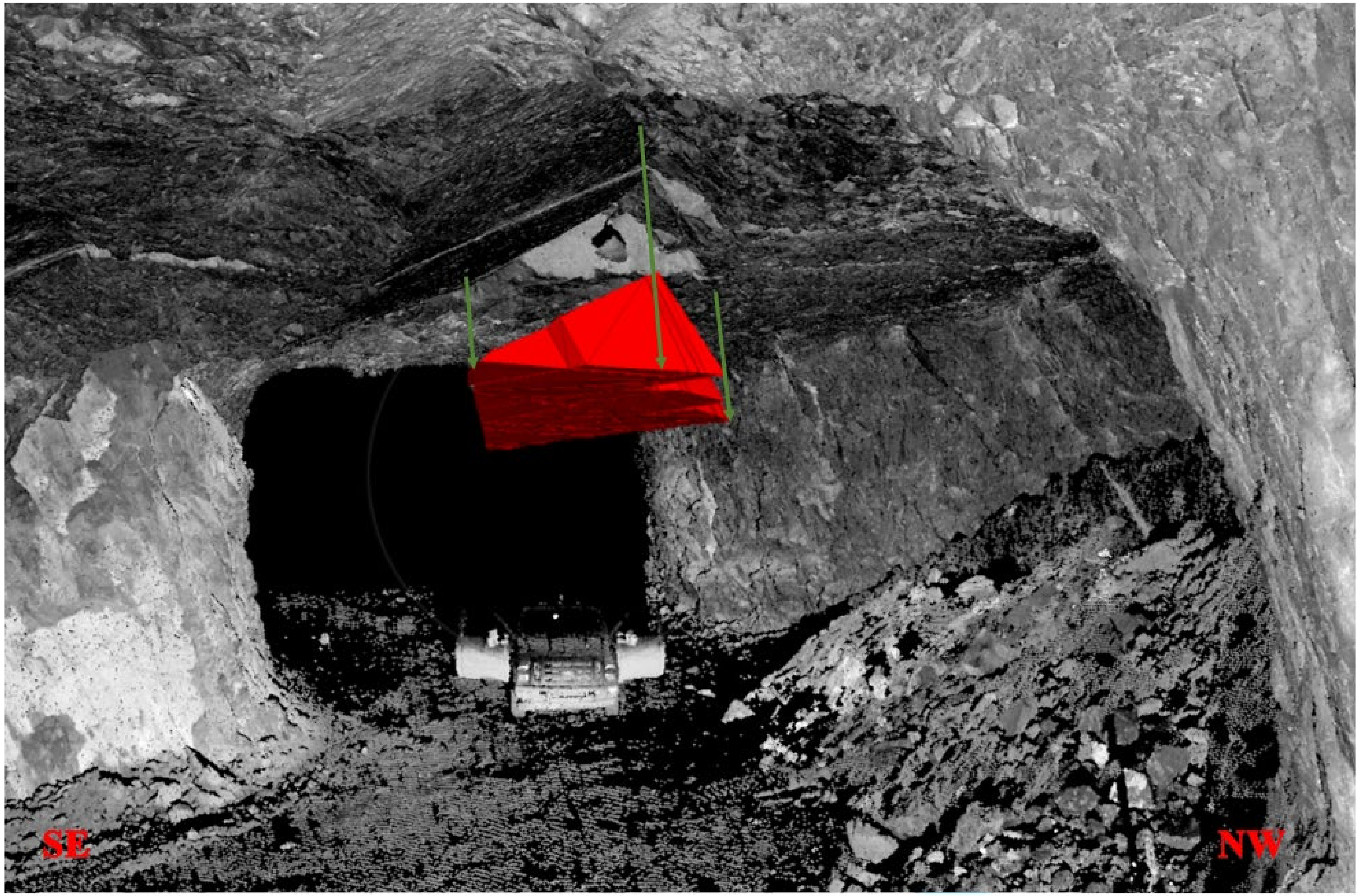

6. CONCLUSIONS

- TLS was proved to be a powerful tool for rock mass characterization.

- An adequate Laser scan project planning allowed
  - to save time during the scanning process
  - reduce errors on the resulting point clouds
  - obtain the necessary information required for virtual discontinuity mapping.
- DEM software such as 3DEC is a powerful tool to interpret and analyze structurally controlled instability in underground excavations.

- TLS and DEM were successfully integrated to estimate the probability of rock falls in an underground excavations

6. CONCLUSIONS

- A clear understanding of the geological model of the site is important in order to improve the results from virtual discontinuity mapping and the fractured rock mass model.
- A rigid block model assumption yielded results that agreed with the field observations and laser scanning results.
- A stochastic Discrete element modeling approach was selected for the analysis due to the stochastic nature of DFNs.
- The present methodology can be used as a method for rock fall hazard identification in underground limestone mines. It can be easily integrated into a groundcontrol risk management system.
- The case study mine offered an ideal environment to apply both technologies.

QUESTIONS?

REFERENCES

- Cacciari, P. and Futai, M. (2017). "Modeling a shallow rock tunnel using terrestrial laser scanning and discrete fracture networks." Rock Mechanics and Rock Engineering 50(5): 1217–1242.
- Cacciari, P., Morikawa, D., and Futai, M. (2015). "Modelling a railway rock tunnel using terrestrial laser scanning and the distinct element method." In: Proceedings of the 8th South American Congress on Rock Mechanics. Lisbon, Portugal: International Society for Rock Mechanics and Rock Engineering, pp. 101–108.
- DiCarlo. (2013). 3D Laser Scanning Set Up. DiCarlo Precision Instrument, Inc.
- Esterhuizen, G. S., Dolinar, D. R., Ellenberger, J. L., and Prosser, L. J. (2011). Pillar and Roof Span Design Guidelines for Underground Stone Mines. Information Circular 9526. Pittsburgh, PA: National Institute for Occupational Safety and Health (NIOSH). Office of Mine Safety and Health Research.
- FARO. (2011). FARO FOCUS 3D Manual. FARO Technologies, Inc.
- FARO. (2018). SCENE. FARO Technologies, Inc.
- Fekete, S. (2010a). "Geotechnical and operational applications for 3-dimensional laser scanning in drill and blast tunnels." Tunnelling and Underground Space Technology 25(5): 614–628.
- Fekete, S. (2010b). Geotechnical Applications of LIDAR for Geomechanical Characterization in Drill and Blast Tunnels and Representative 3-Dimensional Discontinuum Modelling. Thesis. Kingston, Ontario: Queen's University, pp. 296.
- Fekete, S. and Diedrichs, M. (2013). "Integration of three-dimensional laser scanning with discontinuum modelling for stability analysis of tunnels in blocky rockmasses." International Journal of Rock Mechanics and Mining Sciences 57: 11–23.
- Feng, X.-T., & Hudson, J. (2011). Rock Engineering Design. London: CRC Press/Balkema.
- Hudson, J., & Feng, X.-T. (2015). Rock Engineering Risk. London: CRC Press/Balkema.
- Hudson, J. and Harrison, J. (2000). Engineering Rock Mechanics: An Introduction to the Principles. New York, NY: Elsevier, pp. 456.

REFERENCES

- ISRM. (1978). "Suggested methods for the quantitative description of discontinuities in rock masses." International Society for Rock Mechanics, pp. 49.
- Jing, L., & Stephansson, O. (2007). Fundamentals of Discrete Element Methods for Rock Engineering Theory and Applications. Amsterdam: ELSEVIER.
- Lato, M., Diederichs, M., Hutchinson, D., and+ Harrap, R. (2009). "Optimization of LiDAR scanning and processing for automated structural evaluation of discontinuities in rock masses." International Journal of Rock Mechanics and Mining Sciences 46(1): 194–199.
- Maptek. (2018). I-Site Studio. Golden, CO: Maptek Pty Ltd.
- Martin, C., Kaiser, P., & Christiansson, R. (2003). Stress, instability and design of underground excavations. *Rock Mechanics and Mining Sciences*, 1-21.
- Monsalve, J., Baggett, J., Bishop, R., and Ripepi, N. (2018). "A preliminary investigation for characterization and modeling of structurally controlled underground limestone mines by integrating laser scanning with discrete element modeling." Forthcoming In: Proceedings of the North American Tunneling Conference. Englewood, CO: Society for Mining, Metallurgy & Exploration.
- MSHA. (2016). Accident Injuries Data Set. U.S. Department of Labor, Mine Safety and Health Administration (MSHA).
- Pierce, M. (2017). An Introduction to Random Disk Discrete Fracture Network (DFN) for Civil and Mining Engineering Applications. ARMA e-Newslatter 20, 3-8.
- Rocscience. (2018). Dips. Toronto, Ontario: Rocscience Inc.
- Slaker, B. A. (2015). Monitoring Underground Mine Displacement Using Photogrammetry and Laser Scanning. PhD Dissertation. Blacksburg, VA: Virginia Polytechnic Institute and State University, pp. 155.

5.1. LASER SCANNING - OPERATIONAL CONDITIONS

Scan	Resolution		Quality	Real Scan time [hh:mm:ss]	Point Count	Average Point Cloud Density [Points/cm^2]	Overall Rating
	Millions of Points/Scan						
S-006	44.4	1/4	1x	0:05:12	38,103,388	11.42	5.04
S-007	44.4	1/4	2x	0:06:06	41,229,797	12.48	4.31
S-008	44.4	1/4	3x	0:07:53	41,684,133	12.64	3.36
S-009	44.4	1/4	4x	0:11:28	41,229,797	12.66	2.34
S-010	28.4	1/5	2x	0:05:27	26,273,301	8.06	4.79
S-011	28.4	1/5	3x	0:06:36	26,573,225	8.13	3.96
S-012	28.4	1/5	4x	0:08:54	26,630,099	7.97	2.95

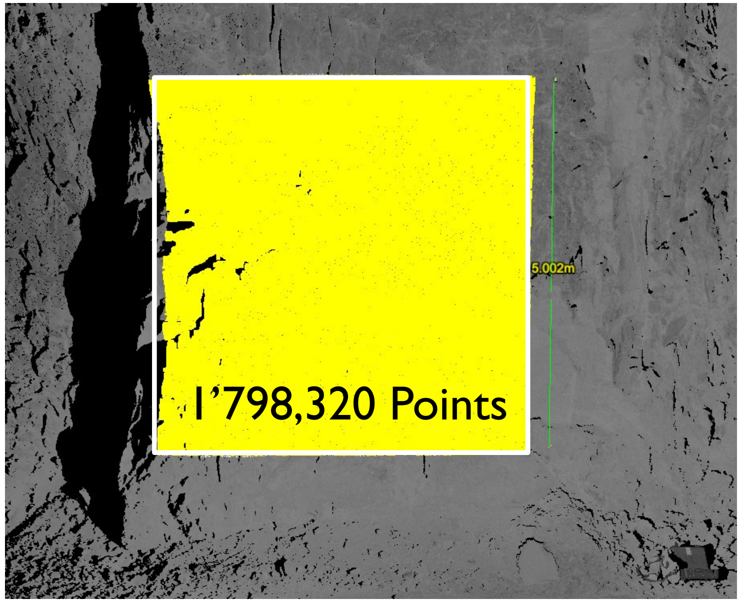

Point Cloud Densities for Structural Mapping	
Author	**Point cloud density**
Lato, Diedrichs, Hutchinson and Harrap, 2009	4 points/cm^2
Cacciari & Futai, 2017	16 points/cm^2
Monsalve, Baggett, Bishop & Ripepi, 2018	11 points/cm^2

5.1. LASER SCANNING - OPERATIONAL CONDITIONS

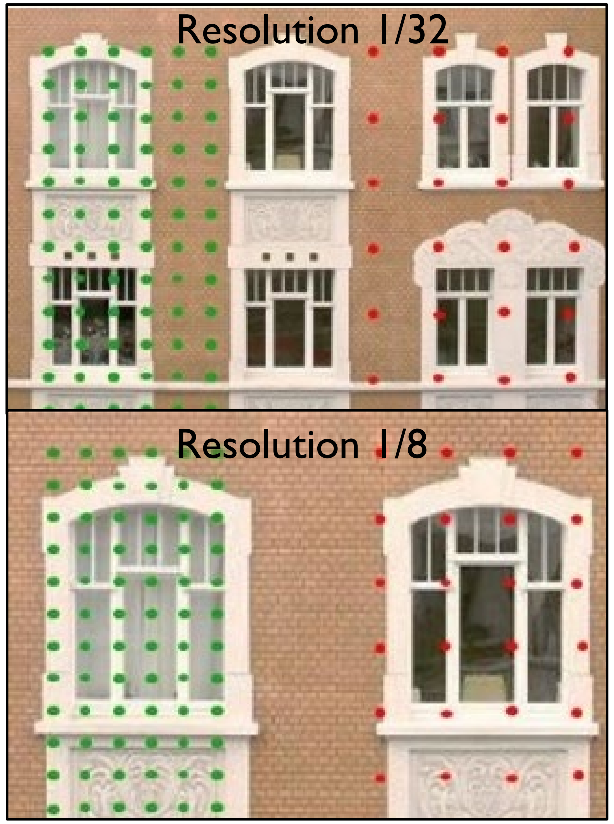

- Laser scanner at a distance of 10m
- Laser scanner at a distance of 20m

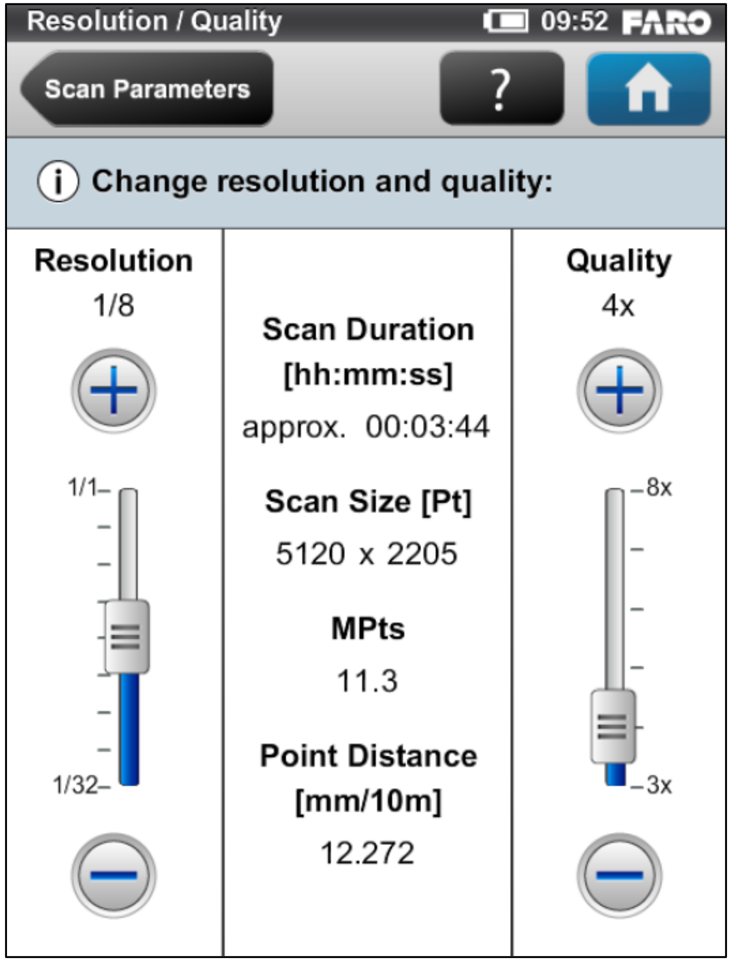

Quality	Observation Time
1 X	1 μs
4 X	8 μs

- Increasing the quality reduces the noise in the distance measurement.
  - ✓ Thickness of a flat object

1 X 4 X

  - ✓ Scan points in far objects

5.1. LASER SCANNING - SCANS REFERENCING

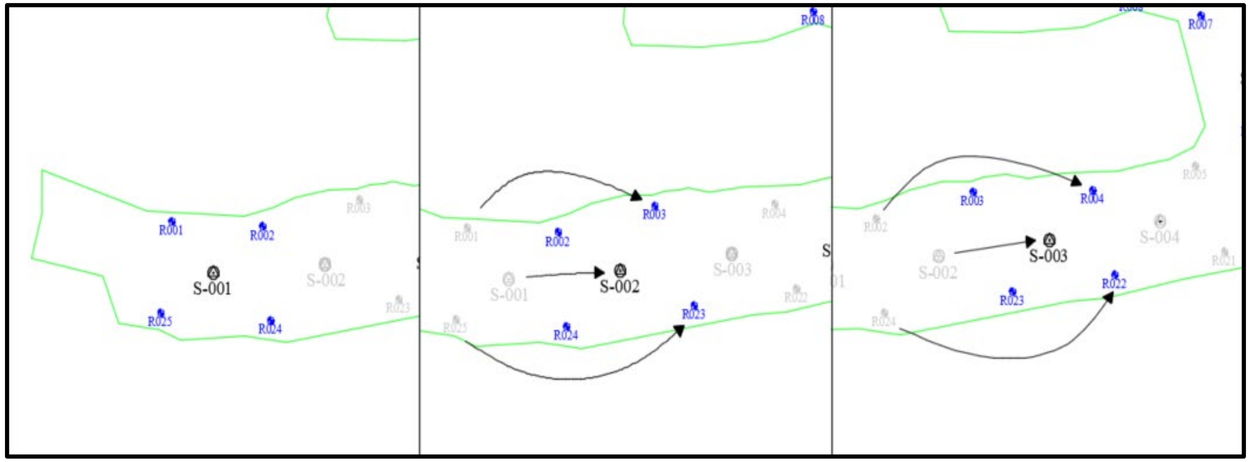

Recommended target spacing

Sphere size	145 mm	Sphere size	230 mm
Resolution Setting	Target Distance (max) in m	Resolution Setting	Target Distance (max) in m
1/16	5	1/16	7
1/10	7	1/10	11
1/8	9	1/8	14
1/5	15	1/5	22
1/4	18	1/4	27
1/2	37	1/2	55
1/1	73	1/1	110

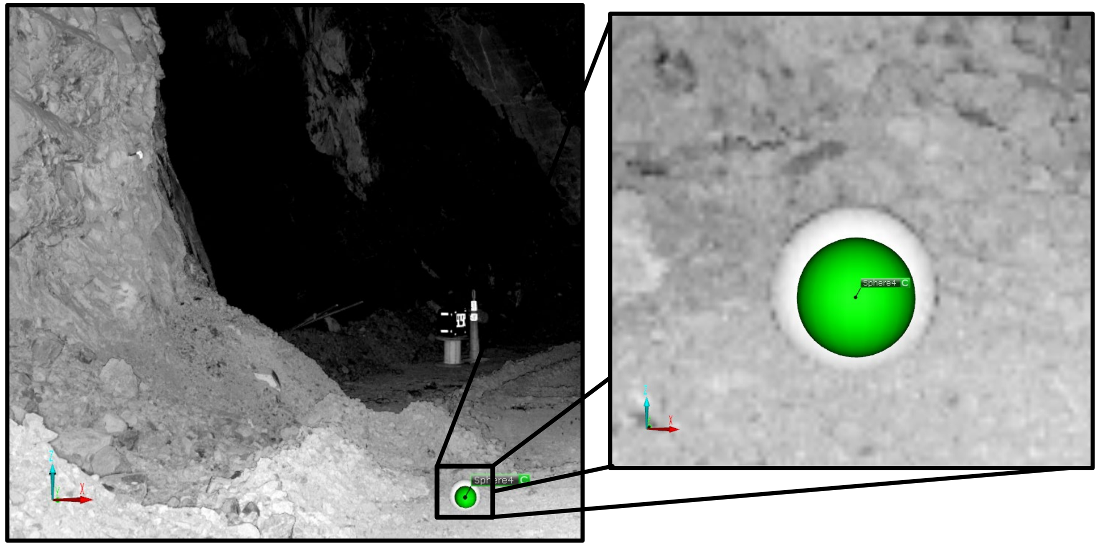

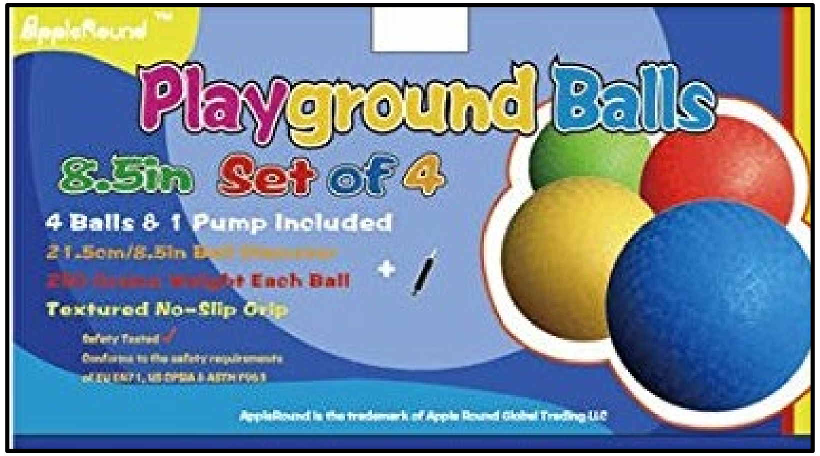

5.1. LASER SCANNING - DATA REGISTRATION

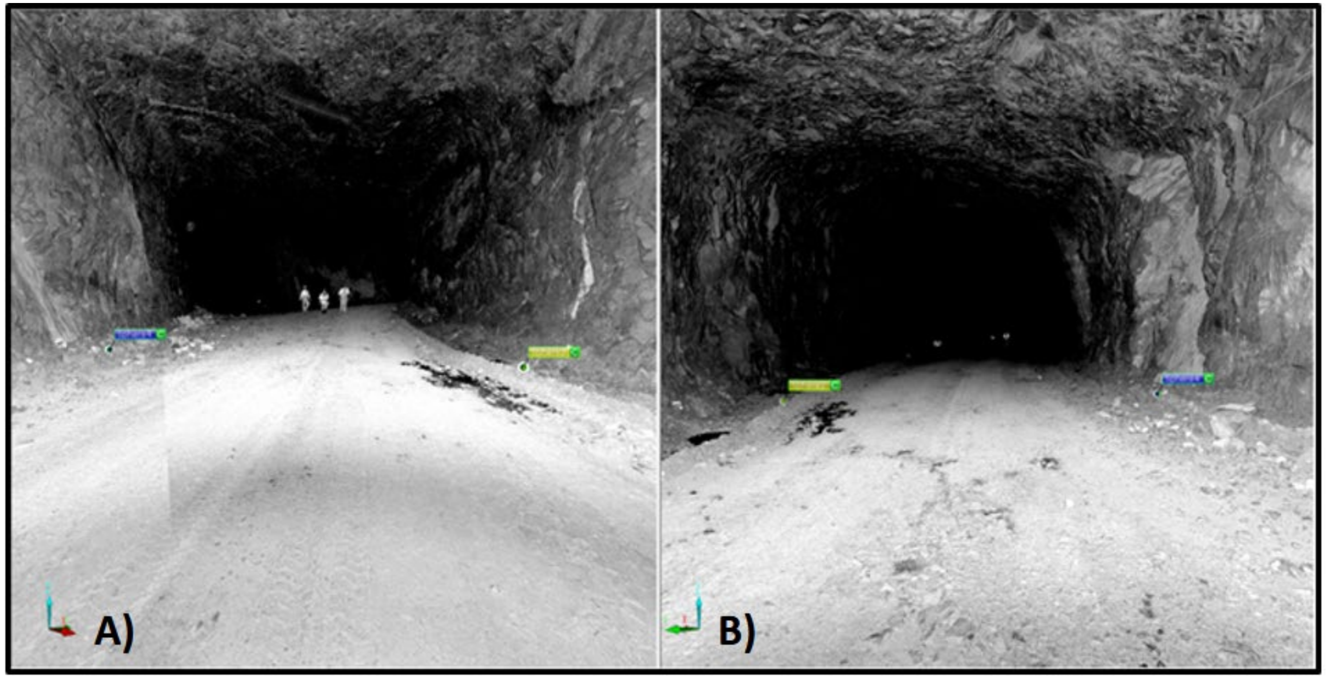

Scan Point Statistics	Obtained Values	Acceptable values	Unacceptable values
Maximum Point Error	6.7 mm	< 8 mm	> 20 mm
Mean Point Error	4.3 mm		
Minimum Overlap	25.2 %	> 25.0 %	< 10.0 %

8. FUTURE WORK

Site Scanning and Discontinuity Characterization

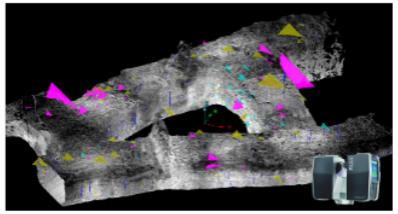

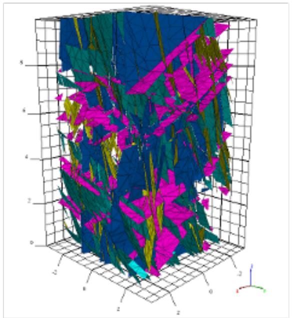

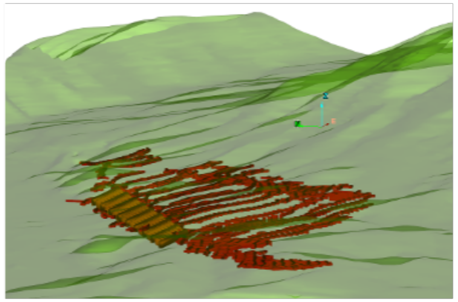

Pillar Strength Determination

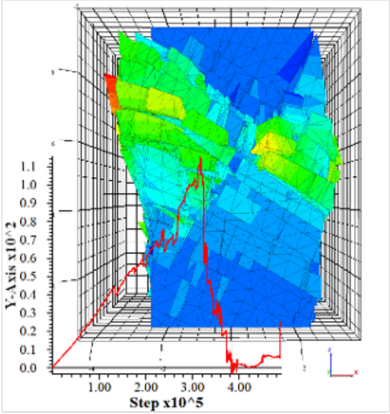

Stress level Estimation

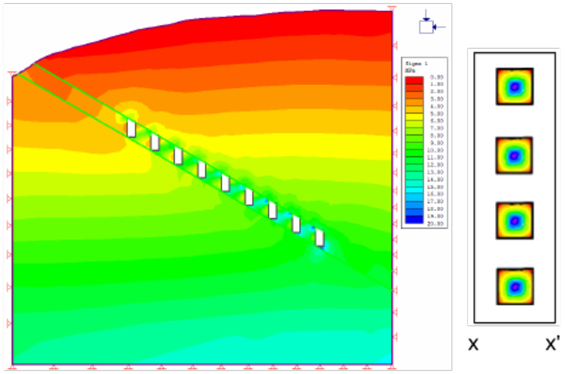

Stochastic Analysis andProbability Distrbution Estimation

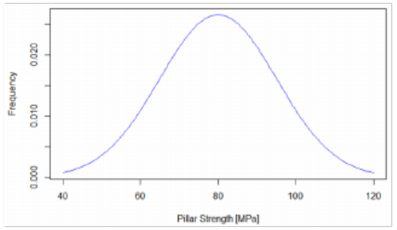

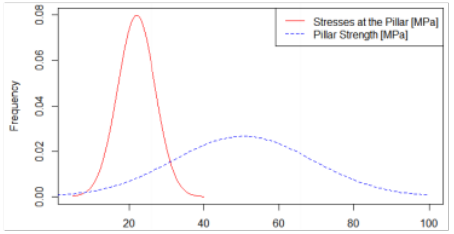

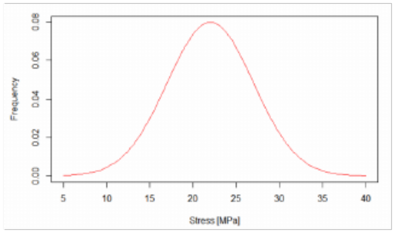

Probability of Failure Estimation

Factor of safety:

$$F.S. = \frac{Strength}{Stress} = \frac{S_p}{\sigma_p}$$

Limit state function:

$$g(\sigma_p, S) = S_p - \sigma_p$$

Failure set:

$$P(failure) = P\{F.S. < 1\} = P\{S_p < \sigma_p\}$$

Reliability index:

$$\beta = \frac{\mu_g}{\sigma_g}$$

Expected value of the limit state function:

$$\mu_g = \mu_{S_p} + \mu_{\sigma_p}$$

Standard deviation of the limit state function:

$$\sigma_g = \sqrt{\sigma_{S_p}{}^2 + \sigma_{\sigma_p}{}^2 - 2\rho_{S_p\sigma_p}\sigma_{S_p}\sigma_{\sigma_p}}$$

Pillar probability of failure:

$$Pf = 1 - \Phi(\beta)$$